

PHYSICAL REVIEW A

GENERAL PHYSICS

THIRD SERIES, VOL. 4, NO. 5

NOVEMBER 1971

M-Subshell Fluorescence Yields and the L_1 - L_3 Radiative Transition at $Z=93$ and 96 from Am^{241} and Cf^{249} Decays*

E. Karttunen,[†] H. U. Freund,[‡] and R. W. Fink

School of Chemistry, Georgia Institute of Technology, Atlanta, Georgia 30332

(Received 9 July 1971)

High-resolution Ge(Li) and Si(Li) x-ray spectrometers and a wall-less anticoincidence multiwire proportional counter were used for coincidence measurements between various K and L x rays and M x rays of Np ($Z=93$) and Cm ($Z=96$) following α decay of Am^{241} and Cf^{249} , respectively. The effect of multiple vacancies in the M shell was taken into account in the determination of the following mean M -subshell fluorescence yields: $\nu_1^M = 0.065 \pm 0.014$, $\nu_2^M = 0.080 \pm 0.029$, $\nu_3^M = 0.062 \pm 0.005$, $\nu_{4,5}^M = 0.065 \pm 0.012 \approx \omega_5^M$ at $Z=93$; and $\nu_1^M = 0.081 \pm 0.016$, $\nu_2^M = 0.068 \pm 0.023$, $\nu_3^M = 0.062 \pm 0.019$, $\nu_4^M = 0.080 \pm 0.006$, and $\nu_{4,5}^M = 0.075 \pm 0.012 \approx \omega_5^M$ at $Z=96$. The close agreement of the various mean M -subshell fluorescence yields with that of the $M_{4,5}$ subshells for each element indicates that Coster-Kronig transitions are very strong in the M shell. Including earlier measurements of mean M -shell fluorescence yields at lower Z , corrected for multiple vacancies, and accepting Bhalla's theoretical calculations of radiative $M_{4,5}$ -subshell widths, one concludes that the nonradiative widths of the $M_{4,5}$ subshells are essentially constant from $Z=76$ to 96 . Comparison of fluorescence yields of the K shell and the L_3 and $M_{4,5}$ subshells at the same energy of the principal radiative transition (i.e., at different values of Z) indicates that the ratio of radiative to Auger widths decreases from the $1s_{1/2}$ to $2p_{3/2}$ state, but remains constant from $2p_{3/2}$ to $3d_{5/2}$. The resolution of the Si(Li) detector was sufficient to separate the radiative transitions from fillings of the $M_{1,2}$ - and $M_{3,4,5}$ -subshell groups, so that from K and L x-ray coincidences with the $M_{1,2}$ group of x rays, it was possible to determine the following quantities: $\omega_1^M + f_{12}^M \omega_2^M = (2.0_{-2.0}^{+3.0}) \times 10^{-3}$ and $(7.5_{-7.5}^{+8.9}) \times 10^{-3}$ at $Z=93$ and 96 , respectively, and $\omega_2^M = (4.6_{-4.6}^{+5.1}) \times 10^{-3}$ at $Z=96$. Thus, about 94% of M_2 -subshell vacancies undergo Coster-Kronig shifts to higher subshells before filling from N and higher major shells occurs. Observation of the radiative L_1 - L_3 transition was made for the first time in the high- Z region, and its intensity is in reasonable agreement with extrapolated theoretical predictions (6–7% of x rays filling L_1 -subshell vacancies). The radiative fraction ω_{13}^L in the Coster-Kronig yield f_{13}^L is found to be about 2% in the region of $Z=93$ – 96 , and $\omega_{13}^L = 0.011 \pm 0.005$ and 0.009 ± 0.005 at $Z=93$ and 96 , respectively. The absolute emission rate of M x rays from Am^{241} was measured with multiwire and single-wire proportional counters, and values are found of $(6.35 \pm 0.60) \times 10^{-2}$ M x rays per α decay and 0.470 ± 0.045 M x rays per L_α x ray. These intensities were used in determinations of efficiency at 3.25 keV of the semiconductor x-ray detectors.

INTRODUCTION

The only modern theoretical calculation of radiative-transition probabilities for transitions to M -shell vacancies is that of Bhalla,¹ but no systematic theoretical calculation has appeared on nonradiative M -shell filling probabilities. Thus, accurate experimental measurements of M -shell and mean M -shell fluorescence yields and Coster-Kronig (CK) transition probabilities are valuable for the further development of theory, as well as for

experimental problems involving M x rays.

Experimental information on M and higher shells is very scarce. A few mean M -shell fluorescence yield measurements have been reported, viz., those for uranium,² gold and lead,³ and bismuth.^{3,4} Coincidences between unresolved L x rays and M x rays of osmium, gold, and lead also have been measured,⁵ in order to determine a mean M -fluorescence yield ω_{LM} in coincidence with L x rays for these elements. Both types of mean M -fluorescence yields, in principle, are dependent on the M - and/

TABLE I. Previous measurements of mean M -shell fluorescence yields. Footnotes refer to method used.

Z Element	$\bar{\omega}_M$	ω_{LM}	Ref.
76 Os		0.016 ± 0.003 ^a	5
		0.013 ± 0.002 ^b	5
79 Au	0.023 ± 0.001 ^c		3
		0.030 ± 0.006 ^a	5
		0.024 ± 0.005 ^b	5
82 Pb	0.029 ± 0.002 ^c		3
		0.032 ± 0.006 ^a	5
		0.026 ± 0.005 ^b	5
83 Bi	0.037 ± 0.007 ^d		4
			3
	0.035 ± 0.002 ^c	0.037 ± 0.007 ^a	5
		0.030 ± 0.006 ^b	5
92 U	0.06 ^e		2

^aFluorescent excitation of the L shell; unresolved L - M x-ray coincidences with NaI(Tl)-gas proportional counter system.

^bSame as Ref. a, but corrected for 20% effect of multiple vacancies (see Ref. 6).

^cFluorescent excitation of the M shell; ionization calculated from photoelectric cross sections and M x rays measured with a proportional counter.

^dRadioactive source, RaD(Pb²¹⁰); M -shell ionization was determined from internal conversion of the 46.5 keV M_1 γ ray and from the L -shell fluorescence yields, and M x rays detected with a proportional counter.

^eFluorescent excitation of the M shell; M x rays detected with a photographic plate.

or L -subshell vacancy distributions and hence on the mode of ionization.⁶ The results of the previous experiments are summarized in Table I.

Modern Ge(Li) and Si(Li) x-ray spectrometers are capable of resolving some individual L - M x-ray lines (e.g., L_3 - M_1 , L_3 - $M_{4,5}$, L_2 - M_4) and K - M x-ray lines (e.g., K - M_2 , K - M_3) in high- Z sources, and this makes possible the use of the coincidence method to investigate various M -subshell fluorescence yields. In the present work,⁷ such measurements were carried out on radioactive sources of Am²⁴¹ and Cf²⁴⁹. For determination of the detection efficiency for M x rays (from 3 to 5 keV) the absolute emission rate of M x rays from Am²⁴¹ decay was measured with a wall-less anticoincidence multiwire proportional counter (MWPC) and a single-wire proportional counter (SWPC).

BASIS OF EXPERIMENTAL METHOD

In a coincidence measurement, gated with L_j - M_i or K - M_i x rays, one is able to isolate the vacancies created in the M_i subshell from other M -shell vacancies and to follow their mode of filling. Absolute counting of M x rays gives the value of the mean M_i -subshell fluorescence yield ν_i^M , or the M -subshell fluorescence yield ω_i^M , depending

on whether the M x-ray spectrum is unresolved or resolved, respectively,

$$\nu_i^M = \frac{1}{\bar{\epsilon}_M(1+m_{ej})} \frac{C_{M(X_j-M_i)}}{C_{X_j-M_i}} \quad (1)$$

or

$$\omega_i^M = \frac{1}{\bar{\epsilon}_{M_i}(1+m_{ej}^X)} \frac{C_{M_i(X_j-M_i)}}{C_{X_j-M_i}}, \quad (2)$$

where $C_M(X_j - M_i)$ and $C_{M_i}(X_j - M_i)$ are the coincidence counting rates of M and M_i x rays, respectively, corresponding to the gate counting rates $C_{X_j-M_i}$ (where X refers to the K or L shells). The average detection efficiency of M or M_i x rays is $\bar{\epsilon}_M$ or $\bar{\epsilon}_{M_i}$, respectively. The factor $(1+m_{ej}^X)$ gives a correction for multiple M -shell or M_i -subshell vacancies arising from electronic processes. This *electronic* vacancy multiplication starts from one original K - or L -shell vacancy and in the high- Z region is due to CK transitions L_1 - $L_3M_{3,4,5}$ and L_2 - $L_3M_{4,5}$ and to certain K Auger processes. Owing to the smallness of the K -shell Auger yield a_K (0.025 at $Z=96$), the multiplication arising from Auger transitions can be neglected when high- Z sources are measured. Then it can be readily shown⁷ that the electronic vacancy multiplication term m_{ej}^X for the K and L shells in the unresolved case [Eq. (1)] is given by $m_e^K = m_{e1}^L = m_{e2}^L = 0$,

$$m_{e3}^L = \frac{1}{V_3} \left\{ \left[\frac{I(L_1-L_3M)}{I(L_1-L_3X)} f_{13} + \frac{I(L_2-L_3M)}{I(L_2-L_3X)} f_{12}f_{23} \right] N_1 + \left[\frac{I(L_2-L_3M)}{(L_2-L_3X)} f_{23} \right] N_2 \right\}, \quad (3)$$

where $I(L_i-L_jM)$ is the intensity of the transition indicated and $I(L_i-L_jX)$ is the total intensity of all L_i-L_jX transitions with X meaning any possible subshell. The quantities f_{12} , f_{13} , and f_{23} are the L -shell CK yields; N_1 and N_2 are the number of original L_1 - and L_2 -subshell vacancies (before L -shell CK transitions but including the vacancies shifted from the K shell to the L shell), respectively; and V_3 is the final number of L_3 -subshell vacancies (after L -shell CK transitions). Numerical evaluation⁷ gave the values 0.46 ± 0.10 and 0.29 ± 0.08 for m_{e3}^L in the decays of Am²⁴¹ and Cf²⁴⁹, respectively.

Another class of multiple vacancies is created in cascading nuclear processes in radioactive decay. Calculation of the *nuclear* cascading multiplication is more difficult and less accurate owing to lack of information on the nonradiative L -shell transition rates and uncertainties in the vacancy distributions. The correction can, how-

ever, be made experimentally by gating on X_j - N , O x-ray lines, where nuclear cascading is the only source of true coincidences. Since none of the L_1 - N , O or L_3 - N , O lines is adequately separated for gating purposes, the correction was measured for x rays emitted in transitions to the L_2 subshell with L_2 - N_4 x-ray gating, and the correction for x-ray transitions filling L_1 and L_3 vacancies was made by using the calculated ratios⁷ $m_{n1}^L : m_{n2}^L : m_{n3}^L = 0.91 : 1 : 1.07$ for Am^{241} and $1.04 : 1 : 1.11$ for Cf^{249} . In Eqs. (1) and (2), coincidence rates experimentally corrected for nuclear cascades must be used.

EXPERIMENTAL PROCEDURE AND EVALUATION OF DATA

Radioactive Sources

The Am^{241} sources were made by droplet evaporation from a carrier-free and solids-free $\text{Am}(\text{NO}_3)_3$ solution on thin (0.9 mg/cm^2) aluminized Mylar foil. The sources were 2–3 mm in diameter and barely visible. They were covered with a Krylon-spray coating of $150\text{--}300 \text{ } \mu\text{g/cm}^2$ to prevent loss of activity from α recoils. The Am^{241} sources ranged in strength from 0.45 to $1.53 \text{ } \mu\text{Ci}$.

The Cf^{249} source which was received as a loan from the Transuranium Research Laboratory at Oak Ridge National Laboratory had been made by electrodeposition on a 0.13-mm-thick beryllium disk. The active diameter of the radioactive source was 0.94 cm and its activity was $16 \text{ } \mu\text{Ci}$ ($4 \text{ } \mu\text{g}$). This source produced a few neutrons from the $\text{Be}^9(\alpha, n)$ reaction, but their presence was not disturbing.

Detectors and Electronic Circuits

Two different coincidence systems were used, a Ge(Li)-Si(Li) system and a wall-less anticoincidence MWPC-Ge(Li) system. The K and L x-ray spectra were detected with Ge(Li) x-ray spectrometers. The one used for gating, ORTEC Model 8113-08, gives a resolution of 436 eV full width at half-maximum (FWHM) at 6.4 keV, and the one used in the MWPC-gated experiment, ORTEC Model 8013-08, 343 eV FWHM at 6.4 keV. A Si(Li) x-ray spectrometer, Kevex Model 300/SN-196, with a resolution of 260 eV FWHM at 6.4 keV, was used for detection of the M x-rays. Characteristics of each of these detectors have been described previously.⁸⁻¹⁰

The efficiency of the Si(Li) spectrometer decreases rapidly below about 9 keV, which makes it difficult to determine its efficiency in the M x-ray region of Np and Cm (3–5 keV) by extrapolation from higher energies. Lack of intensity-calibrated standard x-ray sources below 10 keV, on the other hand, prevents direct efficiency

measurements in this region. For these reasons, a MWPC was built,⁷ the efficiency of which can be accurately determined.

The electronic circuit used in the Ge(Li)-Si(Li) coincidence system was essentially the same as previously described¹¹ for fast/slow coincidence measurements with threefold routing, except that in the present work, fourfold routing was used in the Am^{241} experiments with a resolving time of 340 nsec. A resolution of 18% FWHM was obtained at 6.4 keV. In measurements with an internal Am^{241} source, the background reduction in anticoincidence operation was more than 90% at the expense of only 40% reduction in the M x-ray peak intensity. The energy windows were selected in two timing single-channel analyzers, in which the coincidences with Ge(Li) pulses also were made.

Details of the construction, electronics, and detection characteristics of the MWPC are given in Ref. 7.

M X-Ray Emission in Decay of Am^{241}

The efficiency of a proportional counter is determined by its dimensions and the photoelectric cross section of the counting gas. The sensitive volume of the wall-less center counter is not, however, well defined and varies with the ratio of high voltages in center and ring counters.⁷ Therefore, the efficiency of the MWPC for Am^{241} M x rays had to be experimentally determined. Since the K x-ray emission rates of Mn^{54} and Co^{57} , 0.251 ± 0.002^6 and 0.558 ± 0.0067^{12} per disintegration, respectively, are accurately known, these nuclides were used as calibration standards.

The M x-ray spectrum from a collimated external Am^{241} source was measured in the MWPC filled with propane to 760 Torr. As the predominant M x-ray peak of Np occurs at 3.25 keV, the linear absorption coefficient of propane at this energy and at 760 Torr is the same as that of 9:1 argon-methane gas at 237 and 150 Torr, respectively, at 5.5 and 6.5 keV for Mn^{54} and Co^{57} K x rays.¹³ The emission rate of Np M x rays can be obtained from the relationship

$$\begin{aligned} C_M(\text{Am}^{241})/I_M(\text{Am}^{241}) &= C_K(\text{Co}^{57})/I_K(\text{Co}^{57}) \\ &= C_K(\text{Mn}^{54})/I_K(\text{Mn}^{54}), \quad (4) \end{aligned}$$

where I_K and I_M are the emission rates of K and M x rays from the indicated sources, respectively, and C_K and C_M are the counting rates (corrected for differences in external absorption) measured at equivalent pressures for the same absorption coefficient μ . As an average of several measurements with the MWPC, and from identical measurements with the SWPC described previously,¹⁴ a value was obtained of (2.15 ± 0.20) M x rays

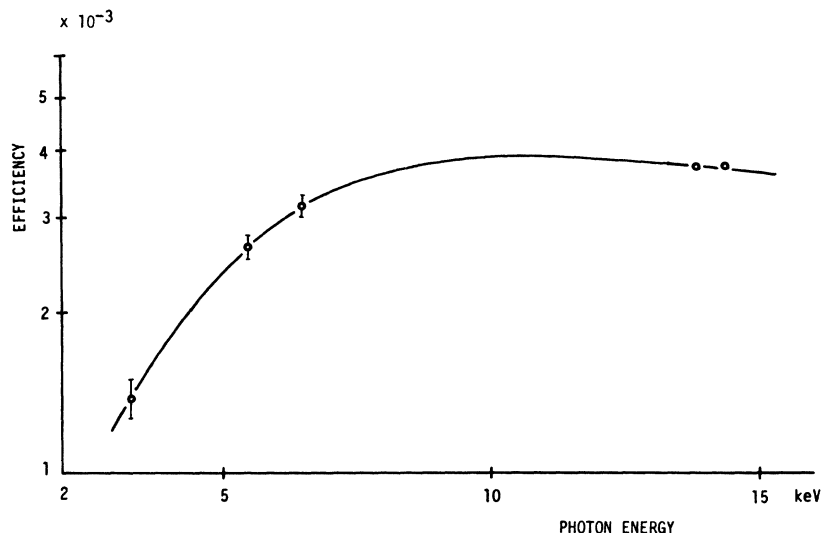


FIG. 1. The detection efficiency of the Si(Li) spectrometer for low-energy photons. The numerical values are for the coincidence geometry used in measurements with a Cf^{249} source. Points at 3.3 and 13.9 keV are from Am^{241} decay; at 6.5 and 14.4 keV, from Co^{57} ; and at 5.5 keV, from Mn^{54} decay.

per min from a 1.53 μCi source of Am^{241} . This gives for the absolute emission of Np M x rays a value of $(6.35 \pm 0.60) \times 10^{-2}$ M x rays/dis of Am^{241} . The ratio of M/L_{α} x-ray emission in Am^{241} decay then is 0.470 ± 0.045 . These numbers are valuable for determining the x-ray efficiencies of semiconductor detectors in the region of 3.25 keV (see Fig. 1).

Coincidence Measurements with Cf^{249} and Am^{241} Sources

A high-resolution singles spectrum of the curium M x-ray region is shown in Fig. 2 with the allowed transition energies marked. This spectrum was taken with a 6-mm-diam \times 3-mm-deep Kevex Si(Li) x-ray spectrometer having resolution

of 180 eV FWHM at 6.4 keV. The most intense peak is composed mainly of transitions filling the $M_{4,5}$ subshells. All x rays which arise from transitions to the $M_{1,2}$ subshells are outside of this peak (on the high-energy side), with the exception of the M_2-N_1 line. On the other hand, the M_3-0 , $P \dots$ group and the line, identified in Fig. 2 as the radiative L_1-L_3 transition on the basis of the transition energy corresponding to the difference in binding between the L_1 and L_3 subshells at $Z=96$, contain the only x rays in this higher-energy region (from 4.5 to 6 keV) that do not belong to transitions filling the $M_{1,2}$ subshells. This gives an opportunity to observe, in a coincidence experiment gated with L_3-M_1 or $K-M_2$ x rays, the

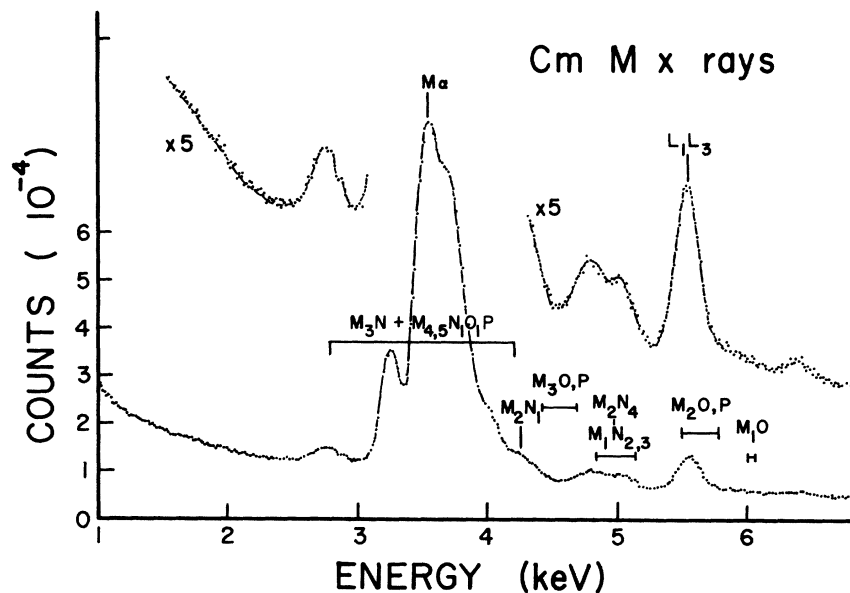


FIG. 2. A singles spectrum of Cm M x-ray region measured with the Si(Li) spectrometer (180 eV FWHM at 6.4 keV).

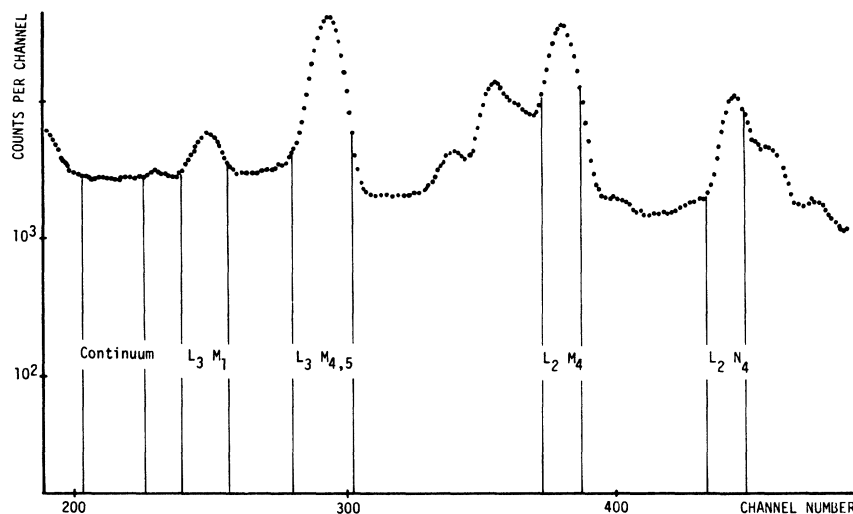


FIG. 3. Gate settings used in the Ge(Li)-gated measurements of the L - M x-ray coincidences with a Cf^{249} source.

direct radiative transitions filling the two lowest M subshells and thus to estimate the quantity $(\omega_1^M + f_{12}^M \omega_2^M)$ or ω_2^M , respectively, and the magnitude of the CK process from $M_{1,2}$ to the $M_{3,4,5}$ subshells. No correction for the "mixing" of the M_2 - N_1 line and the M_3 - O, P group can be made. This probably has no effect on the value of ω_2^M , but may lead to a slightly high estimate for $(\omega_1^M + f_{12}^M \omega_2^M)$.

The gates in the Ge(Li)-Si(Li) coincidence experiments with the Cf^{249} source were set as shown in Fig. 3. In order to be able to correct for the coincidence rate due to the relatively high continuum within the L_1 gate, another gate was set on

the flat spectral region between the germanium $K\alpha$ x ray (9.9 keV) and the L_1 gate. The purpose of gating on the L_2 - N_4 line is to obtain an experimental correction for the nuclear cascading effect.

One chance coincidence run and four separate coincidence runs were made with threefold routing.¹¹ The coincidence-resolving time was doubled in one run to assure that no timing losses of true coincidences occur. A set of four representative coincidence spectra, displaced vertically to ease comparisons, is shown in Fig. 4.

The small difference in the shape of the M x-ray spectrum, regardless of whether the filling of a

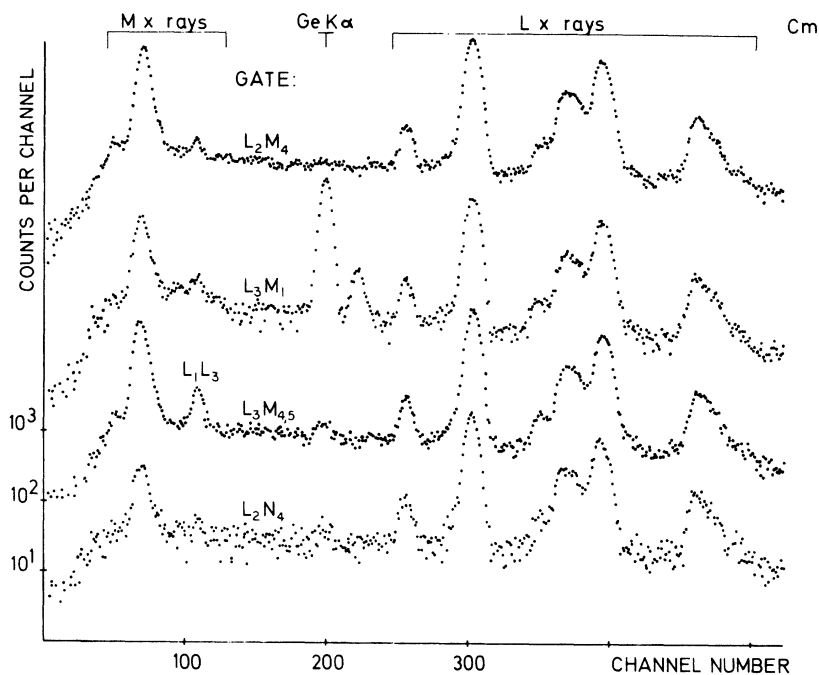


FIG. 4. L x-ray gated coincidence spectra of Cm x rays from Cf^{249} decay, from fourfold routing. The spectra are displaced vertically for ease of comparison.

TABLE II. Gate-counting rates and evaluation of net coincidence counting rates of M x rays, $M_{1,2}$ x rays, and L_1 - L_3 radiative transitions in the Ge(Li)-Si(Li) measurements of L - M x-ray coincidences with a Cf^{249} source.

Gate	M $M_{1,2}$ or L_1L_3	Gross counting rate (counts/min)	Chance correction	Gate correction	Experimental nuclear cascading correction	$C_{M(\text{gate})}$ $C_{M_{1,2}(\text{gate})}$ $C_{L_1L_3(\text{gate})}$ (counts/min)	C_{gate} (counts/min)
L_2 - N_4	M	0.6131 ± 0.0226	0.1625 ± 0.0088			0.4506 ± 0.0242	$6\,047 \pm 44^a$
Continuum	M	0.3523 ± 0.0204	0.0851 ± 0.0046	0.0121 ± 0.0015^b		0.2551 ± 0.0210	$3\,406 \pm 16$
L_2 - M_4	M	3.751 ± 0.034	0.418 ± 0.016		1.181 ± 0.064	2.152 ± 0.075	$16\,797 \pm 80^c$
L_3 - M_1	M	0.6660 ± 0.0120	0.0845 ± 0.0047	0.1792 ± 0.0147^d	0.1152 ± 0.0062	0.2871 ± 0.0205	$1\,708 \pm 66$
L_3 - M_1	$M_{1,2}$	0.0529 ± 0.0143	0.0008 ± 0.0005	0.0186 ± 0.0051^d	0.0090 ± 0.0035	0.0245 ± 0.0147	$1\,708 \pm 66$
L_3 - $M_{4,5}$	M	6.910 ± 0.069	0.697 ± 0.026	0.147 ± 0.015^e	1.970 ± 0.106	4.096 ± 0.129	$26\,240 \pm 150$
L_3 - $M_{4,5}$	L_1L_3	0.670 ± 0.022	0.008 ± 0.006		0.162 ± 0.033	0.500 ± 0.041	$26\,240 \pm 150$

^aCorrected for the presence of 10% of L_1 - N x rays.

^bGate contains 2% of L_3 - M_1 x rays for which a correction has been made.

^cCorrected for the presence of 2% of L_1 - M_3 x rays.

^dGate contains 60% of continuum pulses for which a correction has been made.

^eGate contains 6% of γ - and $L\gamma$ x-ray pulses and 4% of L_2 - M_4 x rays for which correction has been made.

vacancy created in the M_1 or M_5 subshell is followed, indicates the importance of CK transitions in the M shell. The line, identified as an L_1 - L_3 CK x ray in the singles spectrum on the basis of its energy, is seen to be in coincidence with x rays emitted in transitions to the L_3 subshell, particularly with the L_3 - $M_{4,5}$ x rays. This confirms the identification by showing that the line is not due to x rays arising from transitions to $M_{1,2}$ -subshell vacancies, which lie in the same energy region.

Table II gives the evaluation of the corrected coincidence rates corresponding to the net gate counting rates given in the last column. The gate correction arises from the continuum of degraded high-energy gamma rays and x rays and from the overlap of unresolved x-ray lines. A Gaussian fitting analysis performed with a DuPont Model 310 curve-resolving analog computer was used for determination of the overlap, in which procedure good knowledge of transition energies is advantageous. The gross counting rates are averages of values from separate runs and the errors are

1σ standard deviation. Since less than four runs were made with L_2 - M_4 , L_α , and L_2 - N_4 x-ray gates, these error estimates are based on the counting statistics.

The net coincidence rate of M x rays obtained with L_3 - M_1 , L_2 - M_4 , and L_3 - $M_{4,5}$ gates give the mean M -subshell fluorescence yields ν_1^M , ν_4^M , and $\nu_{4,5}^M$ ($\approx 0.1\nu_4^M + 0.9\nu_5^M \approx \omega_5^M$), respectively, through Eq. (1). The analysis of the $M_{1,2}$ x-ray intensity gives the quantity $\omega_1^M + f_{12}^M \omega_2^M$ and the intensity of the radiative component of the L -shell CK yield f_{13} . The detection efficiencies in coincidence geometry are (see Fig. 1) $\bar{\epsilon}_M = (1.61 \pm 0.55) \times 10^{-3}$, $\bar{\epsilon}_{M_{1,2}} = (2.36 \pm 0.12) \times 10^{-3}$, and $\epsilon_{L_1L_3} = (2.70 \pm 0.13) \times 10^{-3}$. The results are discussed below.

The gate positions on the K - M_2 and K - M_3 x-ray lines from Cf^{249} are shown in Fig. 5, and it is clear that the lines do not overlap strongly within the gates (see Table III). The presence of a previously unknown γ ray at 121.5 keV under the K - M_2 x-ray line in Cf^{249} decay contributes about 5% to the gross intensity of this x-ray peak.¹⁵

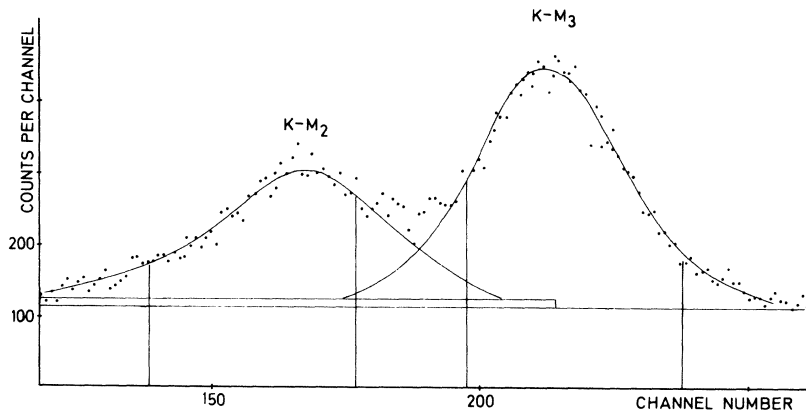


FIG. 5. Gate settings in the $K\beta'$ group in the Ge(Li)-gated measurements of K - M x-ray coincidences with the Cf^{249} source. The relatively high level of the continuum of degraded pulses and the good separation of the K - M_2 and K - M_3 peaks is illustrated.

TABLE III. Gate-counting rates and evaluation of net coincidence counting rates of M x rays and M_2 x rays in the Ge(Li)-Si(Li) measurements of K - M x-ray coincidences with a Cf^{249} source.

Gate	M or M_2	Gross counting rate (counts/min)	Chance correction	Gate correction	Experimental nuclear cascading (counts/min)	$C_{M_2}^{(gate)}$ (counts/min)	C_{gate} (counts/min)
Continuum	M	0.0854 ± 0.0145					1319.7 ± 1.3
K - N , O	M	0.1019 ± 0.0047	0.0344 ± 0.0045	0.0302 ± 0.0034^a			542.9 ± 1.0
K - M_3	M	0.2280 ± 0.0068	0.0307 ± 0.0031	0.0193 ± 0.0021^b	0.0734 ± 0.0134	0.1046 ± 0.0155	0139.4 ± 9.5
K - M_2	M	0.1551 ± 0.0054	0.0262 ± 0.0025	0.0226 ± 0.0023^c	0.0449 ± 0.0083	0.0612 ± 0.0103	536.9 ± 14.7
K - M_2	M_2	0.0069 ± 0.0033	0.0002 ± 0.0002	0.0008 ± 0.0006^c	0.0004 ± 0.0003	0.0055 ± 0.0034	536.9 ± 14.7

^aGate contains 53% of degraded γ pulses for which a correction has been made.

^bGate contains 26% of γ pulses, 1.2% of K - N , O and

0.6% of K - M_2 x rays for which corrections have been made.

^cGate contains 39% of γ pulses, 1.7% of K - N , O and

5.3% of K - M_3 x rays for which corrections have been made.

Additional gates were set on the $K\beta_2'$ x-ray group (K - N , O ...) in order to measure the nuclear cascading correction, and on the continuum above this group in order to get the continuum coincidence rate in the $K\beta_2'$ gate. The measurements by gating with K - M x rays give values for the quantities ν_2^M and ν_3^M , thus completing the series of mean M -subshell yields obtained from the L x-ray gated measurements.

One coincidence and one chance coincidence run were measured with each gate. Although the counting time was 11 days, the statistics are poor owing to the low efficiency of the gate detector at energies over 100 keV and to the small intensity of the K x rays. Evaluation of the net coincidence rates is given in Table III. The error limits are determined from counting statistics (1 standard deviation).

The Ge(Li) spectrum of the L x rays of neptunium is slightly less well separated than that of curium. For the purpose of gating, the difference is insig-

nificant and thus the procedure described above for the L - M x-ray coincidence measurements with the Cf^{249} source was repeated with an Am^{241} source. Evaluation of the net coincidence rates is given in Table IV. In the L_3 - M_1 gated spectrum, the overlap of L_1 - L_3 x rays with the weak group of M x rays filling $M_{1,2}$ -subshell vacancies makes the direct evaluation of the latter intensity difficult. Therefore, the contribution of the L_1 - L_3 x ray was first removed by subtracting the L_3 - $M_{4,5}$ -gated spectrum, normalized to the same gate-counting rate, from the L_3 - M_1 -gated spectrum. This process also corrects for chance coincidences and for nuclear cascading. The detection efficiencies in coincidence geometry are $\bar{\epsilon}_M(\text{Np}) = (8.86 \pm 0.80) \times 10^{-3}$, $\bar{\epsilon}_{M_{1,2}}(\text{Np}) = (1.10 \pm 0.10) \times 10^{-2}$, and $\epsilon_{L_1 L_3}(\text{Np}) = (1.12 \pm 0.06) \times 10^{-2}$. Since no K -shell ionization takes place in the decay of Am^{241} , K x-ray gating cannot be used to give the quantities ν_2^M and ν_3^M in this case. Neither is gating on the weak unresolved L x-ray lines feeding $M_{2,3}$ -subshell

TABLE IV. Gate-counting rates and evaluation of net coincidence counting rates of M x rays, $M_{1,2}$ x rays, and L_1 - L_3 radiative transitions in the Ge(Li)-Si(Li) measurements of L - M x-ray coincidences with Am^{241} source.

Gate	M or $M_{1,2}$ $L_1 L_3$	Gross counting rate (counts/min)	Chance correction	Gate correction	Experimental nuclear cascading correction	$C_{M_{1,2}}^{(gate)}$ $C_{L_1 L_3}^{(gate)}$ (counts/min)	C_{gate}
L_2 - N_4	M	1.626 ± 0.036	0.058 ± 0.006	0.046 ± 0.005^a		1.522 ± 0.037	4177 ± 40^b
Continuum	M	1.561 ± 0.082	0.033 ± 0.004	0.035 ± 0.004^c		1.493 ± 0.083	2998 ± 16
L_2 - M_4	M	11.825 ± 0.272	0.168 ± 0.020	0.042 ± 0.004^d	4.550 ± 0.111	7.065 ± 0.295	12934 ± 137^e
L_3 - M_1	M	1.793 ± 0.036	0.031 ± 0.004	0.735 ± 0.039^f	0.333 ± 0.008	0.693 ± 0.055	827 ± 34
L_3 - M_1	$M_{1,2}$	0.161 ± 0.010		0.052 ± 0.008^g		0.018 ± 0.014	827 ± 34
L_3 - $M_{4,5}$	M	16.797 ± 0.536	0.132 ± 0.015	0.294 ± 0.016^h	4.915 ± 0.121	11.456 ± 0.555	13713 ± 80
L_3 - $M_{4,5}$	$L_1 L_3$	1.529 ± 0.092	0.008 ± 0.002		0.296 ± 0.050	1.225 ± 0.105	13713 ± 80

^aGate contains 8% of degraded γ pulses for which correction has been made.

^bCorrected for the presence of 13% of L_1 - N x rays.

^cGate contains 2% of L_3 - M_1 x rays for which correction has been made.

^dGate contains 3% of γ pulses and 5% of L_2 - γ and L_3 - $0_{4,5}$ x rays for which correction has been made.

^eCorrected for the presence of 5% of L_1 - M_3 x rays for which correction has been made.

^fGate contains 64% of continuum pulses for which correction has been made.

^gGate contains 3% of γ pulses, 2% of L_2 - γ and 4% of L_2 - M_4 x rays for which correction has been made.

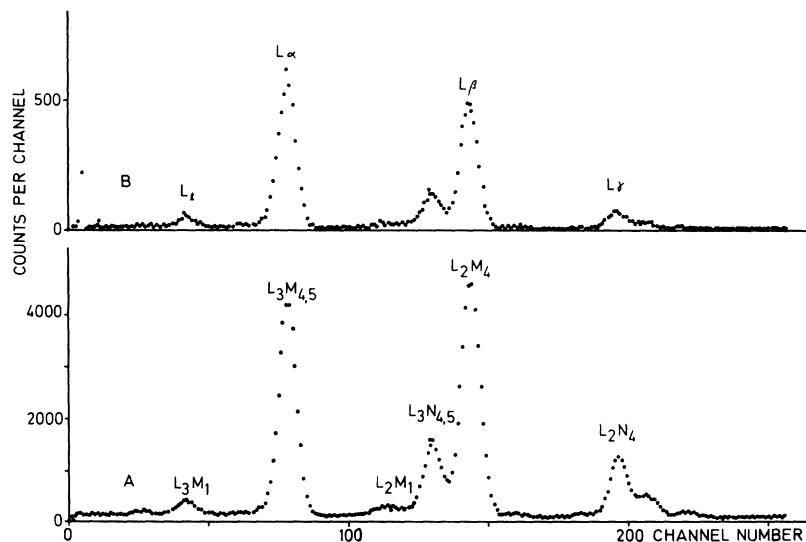


FIG. 6. A free run (A) and an M x-ray MWPC-gated coincidence L x-ray spectrum (B) of Np x rays from Am^{241} decay.

vacancies feasible. Coincidence rates between M x rays and such L x rays can be obtained more easily when the M x rays are used for gating and the intensities of L x-ray lines are analyzed by curve resolving. Equation (1) for mean subshell fluorescence yields must be thus modified to give

$$\nu_i^M = \left[\frac{1}{\bar{\epsilon}_M(1+m_{oi})} \right] \left[\frac{C_{L_j M_i(M)}}{C_{L_j M_i}} \right], \quad (5)$$

and the counting rates of the L_j - M_i x ray must be determined both in the coincidence $C_{L_j M_i(M)}$ and the singles spectra $C_{L_j M_i}$. These kind of measurements were performed with an Am^{241} source and with the MWPC as the gate detector. These measurements also serve as a fairly independent test of the results of the Ge(Li)-Si(Li) experiments. A second gate in the region 5.6–8.5 keV gives the coincidence rate due to the continuum within the M x-ray gate. The coincidence spectrum of L x rays from Am^{241} measured with the Ge(Li) detector is shown in Fig. 6, together with a "free

run" (singles) spectrum. The results of the curve-resolving analysis of the two spectra are given in Table V, which also gives the evaluation of the net coincidence rate $C_{L_j M_i(M)}$. Errors are estimated from the reproducibility of separate successive analyses. Known transition energies were used to advantage in the analyses, but owing to the energy dependency of the linewidth, adequate accuracy could be obtained only for the main components in the complex groups. Thus, for example, the accuracy of the L_1 - N and L_3 - N x-ray lines was not adequate for use in determination of the nuclear cascading correction which, therefore, was determined from the L_2 - N_4 line, as previously described. With anticoincidence operation of the MWPC, the efficiency in detection of the M x rays, $\bar{\epsilon}_M$, in Eq. (5) was $(1.45 \pm 0.14) \times 10^{-2}$, as deduced on the basis of the measured M x-ray emission rate.

RESULTS AND DISCUSSION

The low intensity of x rays emitted in transitions

TABLE V. Evaluation of net coincidence counting rates of L x rays in the MWPC-Ge(Li) measurements of M - L x-ray coincidences with Am^{241} source and the respective rates in the "free run" spectrum.

L x ray $L_j M_i$	Gross counting rate (counts/min)	Chance correction	Gate correction	Experimental nuclear cascading correction	$C_{L_j M_i(M)}$ (counts/min)	$C_{L_j M_i}$
L_2 - N_4	0.239 ± 0.012	0.079 ± 0.001	0.016 ± 0.003		0.139 ± 0.013	183 ± 10
L_2 - M_4	1.681 ± 0.042	0.324 ± 0.005	0.037 ± 0.007	0.604 ± 0.054	0.716 ± 0.069	787 ± 20
L_3 - M_1	0.123 ± 0.005	0.017 ± 0.002	0.002 ± 0.002	0.032 ± 0.003	0.072 ± 0.006	41.8 ± 0.5
L_3 - $M_{4,5}$	1.981 ± 0.011	0.303 ± 0.006	0.043 ± 0.018	0.565 ± 0.051	1.070 ± 0.055	735.3 ± 1.0
L_1 - M_2	0.308 ± 0.022	0.054 ± 0.001		0.100 ± 0.009	0.151 ± 0.024	130 ± 10
L_2 - M_1	0.057 ± 0.006	0.012 ± 0.002	0.001 ± 0.001	0.022 ± 0.002	0.023 ± 0.007	28.4 ± 3.0

TABLE VI. Summary of the results on the radiative filling of $M_{1,2}$ -subshell vacancies of Np ($Z=93$) and Cm ($Z=96$).

	$\omega_1^M + f_{12}^M \omega_2^M$	ω_2^M
Np	$(2.0_{-0.2}^{+0.1}) \times 10^{-3}$	
Cm	$(7.5_{-0.7}^{+0.8}) \times 10^{-3}$	$(4.6_{-0.6}^{+0.5}) \times 10^{-3}$

to the $M_{1,2}$ subshells in the high-resolution coincidence spectra gated with L_3 - M_1 and K - M_2 x rays indicates the smallness of the subshell fluorescence yields ω_1^M and ω_2^M . The similarity of the shape of these spectra compared with spectra gated with L_3 - $M_{4,5}$ x rays, on the other hand, is a visual indication of the high probability for a vacancy to shift from the $M_{1,2}$ to the $M_{4,5}$ subshells. A quantitative estimate for ω_2^M of curium is obtained from the K - M_2 -gated spectrum using Eq. (2), while the coincidence rate of $M_{1,2}$ x rays in the L_3 - M_1 -gated spectra gives the quantity

$$\omega_1^M + f_{12}^M \omega_2^M = \left(\frac{1}{\epsilon_{M_{1,2}}} \right) \left(\frac{C_{M_{1,2}(L_3-M_1)}}{C_{L_3-M_1}} \right). \quad (6)$$

The numerical values obtained for Np and Cm are given in Table VI. It appears that ω_1^M and ω_2^M are an order of magnitude smaller than ω_5^M in the region $Z=93-96$.

Table VII gives the values of mean M -subshell fluorescence yields of Np and Cm determined from Eqs. (1) and (5). The error limits are 2 standard deviations and do not include a possible systematic error ($\leq 9\%$) in the efficiency. The dominant error is that due to the large correction for multiple vacancies in coincidence with the gating x ray. This correction in part (electronic vacancy multiplication) had to be computed with inaccurate basic information. Essentially, the same accuracy was achieved regardless of whether the M x rays were detected with the MWPC or with the Si(Li) x-ray spectrometer, and the results obtained with the two methods are in agreement. A quan-

titative estimate of the strength of the CK process can be obtained by assuming that the Auger width Γ_A is nearly constant for various M subshells. The same is true, according to theory,¹ for the radiative width Γ_R . In the M_5 subshell of Cm, $\Gamma_A^5 = 12.3 \Gamma_R^5$, and thus $a_2^M = 0.057$ and

$$\sum_{j=3-5} f_{2j}^M = 0.94_{-0.07}^{+0.06}.$$

This means that 94% of the M_2 -subshell vacancies shift to higher subshells before filling from higher major shells occurs. The high probability of the M -shell CK process, compared to ordinary Auger transitions, has been directly observed¹⁶ at low Z in electron spectra of krypton. Since the CK processes M_3 - $M_{4,5}N$ are energetically possible, it is expected that by analogy these processes dominate the filling of M_3 -subshell vacancies, and that the value of ω_3^M is small. On the other hand, CK transitions M_4 - M_5N are not possible, and f_{45}^M is probably small. Then ω_4^M would be nearly equal to ω_5^M . (No indication of the difference in the shape of the M x-ray spectra between L_2 - M_4 and L_3 - $M_{4,5}$ gatings can, however, be observed with the present resolution.)

The accuracy of the present coincidence experiments was not sufficient to reveal significant differences among various values of ν_i^M . The differences are partly shaded by the presence of vacancies outside the subshell indicated by the gate pulse (due to nuclear and electronic cascading effects). Since the CK yields are of the order of 0.95, it does not seem likely that experiments with sufficient accuracy are feasible even in ideal cases of negligible nuclear cascading (such as in the decay of Np²³⁵). In order to obtain further information of M -subshell yields from x-ray measurements, resolution sufficient to resolve the M x-ray spectrum will be required.

As pointed out above, essentially all of the inner M -subshell vacancies shift to the $M_{4,5}$ subshells before radiative filling occurs. Since, moreover, the quantities ν_4^M and ω_5^M are not very different, the mean M -fluorescence yield is insensitive to the

TABLE VII. Summary of the mean M -subshell fluorescence yields of Np ($Z=93$) and Cm ($Z=96$). Error limits are the 2 standard deviations and do not include a possible systematic error ($\approx 9\%$) in efficiency.

Mean M -subshell fluorescence yield	$Z=93$ Ge(Li)-Si(Li)	$Z=93$ MWPC-Ge(Li)	$Z=96$ Ge(Li)-Si(Li)
ν_1^M	0.065 ± 0.014^a	0.082 ± 0.018	0.081 ± 0.016^b
ν_2^M		0.080 ± 0.029	0.068 ± 0.023
ν_3^M			0.062 ± 0.019
ν_4^M	0.062 ± 0.005	0.063 ± 0.012	0.080 ± 0.006
$\nu_{4,5}^M$ ^c	0.065 ± 0.012^a	0.069 ± 0.012	0.075 ± 0.012^b

^aAbout 24% of the vacancies followed are in the $M_{3,4,5}$ subshells due to $L_{1,2}$ - $L_3M_{3,4,5}$ CK transitions.

^bAbout 18% of the vacancies followed are in the $M_{3,4,5}$ subshells due to $L_{1,2}$ - $L_3M_{3,4,5}$ CK transitions.

^c $\nu_{4,5}^M \approx 0.1\nu_4^M + 0.9\nu_5^M \approx \omega_5^M$.

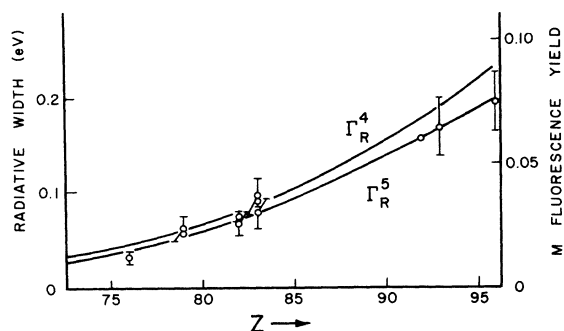


FIG. 7. Experimental M -shell fluorescence yields as a function of atomic number Z , together with a comparison with theoretical radiative widths of the M_4 and M_5 subshells from Ref. 1. It is seen that the M -shell fluorescence yields vary with Z in a manner which follows closely the Z -dependence of the radiative widths $\Gamma_R^{4,5}$.

vacancy distribution and the quantities $\bar{\omega}_M$ and ω_{LM} both are approximately equal to ω_5^M . This explains the similarity of the values of $\bar{\omega}_M$ and ω_{LM} at $Z = 79, 82, \text{ and } 83$ (Table I). This also makes it possible to obtain the Z dependency of the M_5 subshell yield ω_5^M . In Fig. 7, all measured values of $\bar{\omega}_M$, ω_{LM} , and $\nu_{4,5}$ are plotted against Z and compared with the calculated¹ radiative widths of the M_4 and M_5 subshells. It is observed that the measured yields change with Z in a manner following that of the radiative width of the M_5 subshell Γ_R^5 and the M_4 subshell Γ_R^4 . Since

$$\omega_{4,5}^M = \Gamma_R^{4,5} / \Gamma^{4,5} \approx \Gamma_R^{4,5} / \Gamma_{NR}^{4,5}, \quad (7)$$

one concludes that the total width $\Gamma^{4,5}$ and the non-radiative width $\Gamma_{NR}^{4,5}$ of the $M_{4,5}$ subshells are essentially constant with Z in the region $Z = 76-96$.

Figure 8 shows a comparison of the fluorescence yields of the M_5 , L_3 , and K shells, which are not affected by the CK transitions, in the region where the main radiative transitions have comparable energies; i. e., where the $K\alpha$ ($K-L_{2,3}$), $L\alpha$ [$L_3-M_{4,5}$], and $M\alpha$ [$M_5-N_{6,7}$] groups have an energy of 1-4 keV. The curves shown for ω_K ¹⁷ and ω_3^L ^{18,19} are theoretical. In spite of the increase in the radiative width,^{20,21} the fluorescence yield decreases as one goes from K to L_3 and remains unchanged from the L_3 to M_5 subshells at a given transition energy. This indicates that the Auger widths increase at least as rapidly as the radiative widths with in-

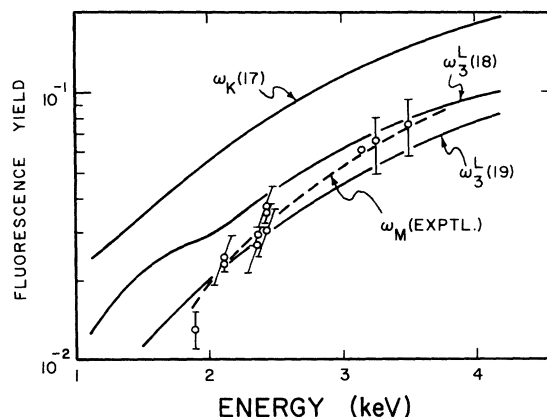


FIG. 8. A comparison of the K -, mean M -, and L_3 -subshell fluorescence yields as a function of transition energy (different Z) of the main radiative component ($K\alpha$, $L\alpha$, $M\alpha$). The lines representing ω_K and ω_3^L are from theory (Refs. 17-19). It is seen that ω_3^L and any of the M -shell fluorescence yields are essentially equal at a fixed transition energy, but that ω_K is considerably larger.

creasing angular momentum of the shell being filled.

The radiative L_1-L_3 transition was observed for the first time in the high- Z region in the course of this work. In the low- Z region ($Z = 11, 12, 13, \text{ and } 16$), the transition has been observed previously with an optical spectrograph.²² The transition was identified both in the Np and Cm x-ray spectra on the basis of its transition energy, and the identification was confirmed in coincidence measurements.

The intensity of the L_1-L_3 x rays as compared with the total intensity of x rays leading to L_3 and L_1 subshells is given in Table VIII. The former value is obtained directly from the $L\alpha$ -gated coincidence spectra. Since the ratio of the total x-ray intensities is $V_3\omega_3/N_1\omega_1$, the latter value can be derived from the former one and from information on the vacancy distribution (see Refs. 6 and 7). The agreement with theory of the transition rates^{20,21} is reasonable.

Because of the existence of a measurable radiative transition between subshells of a major shell, it has been proposed⁶ that the CK yield f_{ij} be considered as the sum of the ordinary non-

TABLE VIII. Intensity of the radiative L_1-L_3 transition at $Z = 93$ and 96 .

Intensity per	Am ²⁴¹ decay		Cf ²⁴⁹ decay	
	Experimental	Theory ^a	Experimental	Theory ^a
L_3 x ray	0.0099 ± 0.0015		0.0081 ± 0.0013	
L_1 x ray	0.058 ± 0.036	0.060	0.041 ± 0.028	0.71

^aExtrapolated from $Z = 92$.

radiative component a_{ij} and a radiative component ω_{ij} . Since $\omega_{13}^L = I_{L_1L_3}/N_1$, Table VIII gives $\omega_{13}^L = 0.011 \pm 0.005$ at $Z=93$ and $\omega_{13}^L = 0.009 \pm 0.005$ at $Z=96$. The radiative component of the total CK yield f_{13}^L thus appears to be about 2% of the total.

ACKNOWLEDGMENT

We are indebted to Dr. R. D. Baybarz of the Transuranium Research Laboratory at Oak Ridge National Laboratory for the source of Cf²⁴⁹.

*Supported in part by the U. S. Atomic Energy Commission.

†Present address: Department of Radiochemistry, University of Helsinki, Unionink. 35, Helsinki, Finland.

‡Present address: Battelle Institute e. V., Frankfurt, West Germany.

¹C. P. Bhalla, *J. Phys.* B **3**, 916 (1970).

²H. Lay, *Z. Physik* **91**, 533 (1934).

³A. A. Konstantinov and T. E. Sazanova, *Bull. Acad. Sci. USSR Phys. Ser.* **32**, 58 (1968).

⁴A. A. Jaffe, *Bull. Res. Council Israel* **3**, 316 (1954); see *Phys. Abstr.* **58**, 360 (1955).

⁵R. C. Jopson, Hans Mark, C. D. Swift, and M. A. Williamson, *Phys. Rev.* **137**, A1353 (1965).

⁶W. Bambynek, B. Crasemann, R. W. Fink, H. U. Freund, Hans Mark, R. E. Price, P. Venugopala Rao, and C. D. Swift, *Rev. Mod. Phys.* (to be published).

⁷E. Karttunen, Ph. D. thesis (Georgia Institute of Technology, 1971) (unpublished).

⁸H. U. Freund, J. S. Hansen, E. Karttunen, and R. W. Fink, in *Proceedings of the International Conference on Radioactivity in Nuclear Spectroscopy* (Gordon and Breach, New York, 1971).

⁹J. S. Hansen, H. U. Freund, and R. W. Fink, *Nucl.*

Phys. **A142**, 604 (1970); **A153**, 465 (1970).

¹⁰D. Nix, J. C. McGeorge, and R. W. Fink (unpublished).

¹¹J. C. McGeorge, H. U. Freund, and R. W. Fink, *Nucl. Phys.* **A154**, 526 (1970).

¹²H. U. Freund and J. C. McGeorge, *Z. Physik* **238**, 6 (1970).

¹³V. M. J. Veigele, E. Briggs, B. Bracewell, and M. Donaldson, Kaman Nuclear Corp., Report No. KN-798-69-2(R), 1969 (unpublished).

¹⁴H. Genz, D. S. Harmer, and R. W. Fink, *Nucl. Instr. Methods* **60**, 195 (1967).

¹⁵W. D. Schmidt-Ott, R. W. Fink, and P. Venugopala Rao, *Z. Physik* **245**, 191 (1971).

¹⁶W. Mehlhorn, *Z. Physik* **187**, 21 (1965).

¹⁷V. O. Kostroun, M. H. Chen, and B. Crasemann, *Phys. Rev. A* **3**, 533 (1971).

¹⁸E. J. McGuire, *Phys. Rev. A* **3**, 587 (1971).

¹⁹M. H. Chen, B. Crasemann, and V. O. Kostroun, *Phys. Rev. A* **4**, 1 (1971).

²⁰J. H. Scofield, *Phys. Rev.* **179**, 9 (1969).

²¹H. R. Rosner and C. P. Bhalla, *Z. Physik* **231**, 347 (1969).

²²T. H. Tomboulion, *Phys. Rev.* **74**, 1887 (1948).

Ground-State Energies of the He Atom and the Li⁺ Ion in the Faddeev Approach

G. Banerji, S. N. Banerjee,* and N. C. Sil

Department of Theoretical Physics, Indian Association for the Cultivation of Science, Calcutta - 32, India

(Received 25 June 1971)

The ground-state energies of the He atom and the Li⁺ ion have been calculated using the Faddeev formalism. For the off-shell two-body collision amplitude (t matrix), Sturmian-function (SF) as well as Coulomb-function representations have been employed. For the He atom, calculations have been performed retaining $1s$, $1s$ and $2s$, and $1s$, $2s$, and $3s$ states in the SF representation for the two-body t matrix, whereas only the $1s$ term has been retained in the mixed-mode (MM) representation. For the Li⁺ ion, computations have been done after retaining terms up to $2s$ in the SF representation and only the $1s$ term in the MM representation. The results obtained by retaining only the $1s$ term are in marked disagreement with the experimental values in both representations. It is noticed that the results for the MM representation are almost as much below the experimental values as those for the SF representation are above. The results for the MM representation are slightly better than those for the SF representation. This is seen more clearly in the case of the Li⁺ ion. The results in the SF representation are found to be in good agreement with the experimental findings after inclusion of the $2s$ term.

I. INTRODUCTION

A rigorous mathematical formulation of the non-relativistic three-body problem with pair interactions has been given by Faddeev.^{1,2} For local po-

tentials, the theory involves the solution of a set of coupled integral equations in at least two continuous variables. In the case of Coulomb potentials, Ball *et al.*³ and Chen *et al.*⁴ have used separable expansions for the off-shell two-body collision amplitude